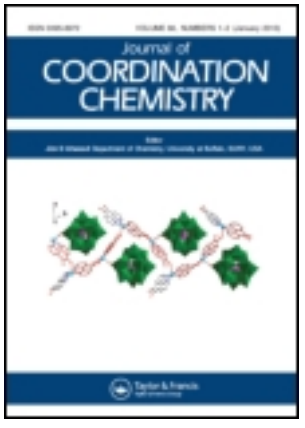

Journal of Coordination Chemistry
Publication details, including instructions for authors and subscription information:
http://www.tandfonline.com/loi/gcoo20

Synthesis, crystal structure, spectroscopic properties, and antimicrobial studies of a zinc(II) complex of p-coumaric acid

M. Kalinowska [a], L. Mazur [b], J. Piekut [a], Z. Rzączyńska [b], B. Laderiere [c] & W. Lewandowski [a]

[a] Division of Chemistry, Bialystok University of Technology, Bialystok, Poland

[b] Department of General and Coordinational Chemistry, Maria Curie-Sklodowska University, Lublin, Poland

[c] Institut des Sciences at Techniques, University of Mont Houy, Le Mont Houy, Valenciennes, France

Accepted author version posted online: 07 Dec 2012.Published online: 19 Feb 2013.

To cite this article: M. Kalinowska, L. Mazur, J. Piekut, Z. Rzączyńska, B. Laderiere & W. Lewandowski (2013) Synthesis, crystal structure, spectroscopic properties, and antimicrobial studies of a zinc(II) complex of p-coumaric acid, Journal of Coordination Chemistry, 66:2, 334-344, DOI: 10.1080/00958972.2012.756480

To link to this article: http://dx.doi.org/10.1080/00958972.2012.756480

Journal of Coordination Chemistry
Vol. 66, No. 2, 20 January 2013, 334–344

Synthesis, crystal structure, spectroscopic properties, and antimicrobial studies of a zinc(II) complex of *p*-coumaric acid

M. KALINOWSKA†, L. MAZUR‡, J. PIEKUT†, Z. RZĄCZYŃSKA‡, B. LADERIERE§ and W. LEWANDOWSKI*†

†Division of Chemistry, Bialystok University of Technology, Bialystok, Poland;
‡Department of General and Coordinational Chemistry, Maria Curie-Sklodowska University, Lublin, Poland;
§Institut des Sciences at Techniques, University of Mont Houy, Le Mont Houy, Valenciennes, France

(*Received 8 August 2012; in final form 13 November 2012*)

The synthesis of the zinc(II) complex of *p*-coumaric acid is described. The chemical formula of the complex as obtained from the single-crystal X-ray analysis is $[Zn_4(C_9H_7O_3)_8(H_2O)_6]\cdot 4(H_2O)$. The compound crystallizes in the triclinic space group *P*-1 with one molecule in the unit cell. There are two crystallographically independent Zn(II) cations in the structure. Zn1 is six-coordinate to three different carboxylate oxygens and three waters in a distorted octahedral geometry, whereas Zn2 ions are connected to four oxygens from four *p*-coumarate anions resulting in tetrahedral geometry. Adjacent cations are connected by bridging carboxylates to form centrosymmetric tetranuclear aggregates. Adjacent molecules are connected by a net of strong O–H···O hydrogen bonds into a 3D supramolecular framework with 1D open channels filled with water molecules. The zinc complex was characterized by infrared spectroscopy and ^{1}H and ^{13}C NMR spectra. The antimicrobial activities of zinc *p*-coumarate toward *Bacillus subtilis*, *Candida albicans*, *Pseudomonas aeruginosa*, *Proteus vulgaris,* and *Staphylococcus aureus* were tested.

Keywords: Zinc(II) complex of *p*-coumaric acid; Synthesis; X-ray crystallography; Spectroscopy; Antimicrobial activity

1. Introduction

p-Coumaric acid (*p*-hydroxycinnamic acid) can be found in a wide variety of edible plants such as peanut, tomato, carrot, garlic, apple, and in many other food products like wines and juices [1]. It is most abundant in nature as an isomer of coumaric acid. *p*-Coumaric acid is an antibacterial, antioxidant and anticancer agent [2, 3]. Studies performed by Wen *et al.* revealed that *p*-hydroxycinnamic acid was bactericidal at pH 4.5 and bacteriostatic at higher pH toward *Listeria monocytogenes* [4]. *p*-Coumaric acid isolated from the stem bark of *Stereospermum zenkeri* possesses antimicrobial activity toward *Bacillus subtilis* (MIC = 18.75 μg/ml, MBC = 37.50 μg/ml) and *Bacillus megaterium* (MIC = 18.75 μg/ml,

*Corresponding author. Email: w-lewando@wp.pl

ISSN 0095-8972 print/ISSN 1029-0389 online
http://dx.doi.org/10.1080/00958972.2012.756480

MBC = 37.50 μg/ml) [5]. The potential use of phenolic extracts as new antimicrobial agents during wine-making, as a total or partial alternative to traditional treatments mainly using sulfur dioxide (SO_2), was discussed by Garcia-Ruiz *et al.* [6]. Significant antibacterial activity activity against *Bacillus cereus* and *Proteus mirabilis* by Rubus honeys was shown by Escuredo *et al. p*-Coumaric acid, as one of the eight isolated phenolic compounds present in this type of honey, was related with some parameters of honey like color [7]. Bodini *et al.* investigated the influence of *p*-coumaric acid on bacterial quorum sensing (tested bacteria: *Escherichia coli*, *Agrobacterium tumefaciens*, *Chromobacterium violaceum*, *Pseudomonas putida* and environmental *Pseudomonas chlororaphis*) [8]. Their results suggested that *p*-coumaric acid might act as a quorum-sensing inhibitor. *p*-Coumaric acid is also a chromophore of the photoactive yellow protein and this molecule has become a model system for studying biological light-induced signal transduction [9]. The study of An *et al.* demonstrated that the compound is a potent and selective inhibitor of human Tyrosinase, and is potentially useful as a hypopigmenting agent [10]. Furthermore, it is capable of inducing neuroprotective effects to a similar extent to that seen with flavonoids, therefore its application in treatment of Parkinson's disease was studied [11]. *p*-Coumaric acid, a major constituent of *Sasa quelpaertensis*, was found to effectively prevent ethanol-induced hepatotoxicity, suggesting that it could be useful for prevention of liver disease caused by alcohol abuse [12]. Numerous examples of biological activity of *p*-coumaric acid and its derivatives could be made.

Synthesis of complexes with biologically active ligand is of great importance due to their potential application in pharmacy, medicine, food industry, catalysis, etc. There is still growing interest in new biologically important coordination compounds as metal binding to some molecules can change their activity and overcome bacterial resistance to antibiotics. Many metal complexes obtained from simple phenolic acids (like *p*-coumarates) [13,14] and more structurally diverse derivatives (like coumarin Schiff bases) [15–19] were screened for antibacterial and antifungal properties. Coumarin is a lacton of coumaric acid. Shiff bases derived from coumarin are useful chelating agents for synthesis of medicinally important metal compounds, which can be more efficient and less toxic than the parent drugs [15–19].

Crystal structures of lanthanum(III) [20], europium(III) [21], cerium(III) [22], cadmium (II) [23], and lead(II) [24] coumarates have been published. The only crystal structure of zinc(II) complex with *p*-coumaric acid reported to date was that containing nicotinamide as a co-ligand [25].

Reasons that force us to search for new antimicrobial compounds are: (1) environmental pollution resulting from the massive use of non-biodegradable antimicrobial compounds or causing the formation of toxic products negatively affect aquatic organisms and then humans; (2) increasing resistance of microbes to the currently used preparations (preservatives, disinfectants, medicines, etc.); (3) occurrence of allergies and the types of diseases caused by frequent contact with the above preparations; and (4) increasing consumer awareness of the need to develop new antimicrobial compounds based on natural compounds of plant origin as an alternative to current preparations.

Therefore, our studies rely on the search for new antimicrobial substances among compounds of natural origin and their metal complexes. Biological properties of chemical compounds depend not only on the structure of the ligand, but also on the type of coordinated metal ion. Chelate compounds may show better antimicrobial activity than simple salts or ligand alone. In our studies, we use several complementary methods to study structures of complexes and ligands, such as infrared spectroscopy (FT-IR), Raman spectroscopy (FT-Raman), nuclear magnetic resonance spectroscopy (NMR), electron

absorption spectroscopy (UV/Vis), single-crystal X-ray analysis, and theoretical calculations (optimization of the structure, the theoretical IR spectra, Raman, NMR, electron charge distribution). These data are used to describe the molecular structure of compounds, and then they are used for correlation with the data describing the antimicrobial properties of compounds. The aim is to obtain information describing the relationship between the structure of compounds and their biological activity (QSAR analysis) which will reduce the time spent on searching for new antimicrobial compounds. In this work, synthesis of a new zinc(II) complex of *p*-coumaric acid as single crystals is described. Diffraction and spectral analysis of the obtained compound was done and antimicrobial activities of zinc *p*-coumarate against *Bacillus subtilis*, *Candida albicans*, *Pseudomonas aeruginosa*, *Proteus vulgaris,* and *Staphylococcus aureus* were tested.

2. Experimental

2.1. *Synthesis*

All reagents were purchased from Sigma-Aldrich Co. and used without purification. Zinc (II) *p*-coumarate was obtained by adding water solutions of $ZnCl_2$ (concentration 0.25 M/L) to water solution of sodium *p*-coumarate (concentration 0.5 M/L) in a stoichiometric ratio 1 : 2. White precipitate occurred. The solution was filtered and the precipitate was dissolved in warm water. The solution was left to cool at room temperature. After a few days, colorless crystals of zinc(II) *p*-coumarate appeared.

2.2. *X-ray crystallography*

The crystallographic measurements were performed on an Oxford Diffraction Xcalibur CCD diffractometer with the graphite-monochromated Mo K_α radiation ($\lambda = 0.71073$ Å). Data sets were collected at 100(2) K using the ω scan technique, with an angular scan width of 0.75°. The programs CrysAlis CCD and CrysAlis Red [26] were used for data collection, cell refinement, and data reduction. A multi-scan absorption correction was applied. The structure was solved by direct methods using SHELXS-97 and refined by full-matrix least-squares on F^2 using SHELXL-97 [27]. Calculations were carried out with the WinGX package program [28]. All non-H atoms were refined with anisotropic displacement parameters. Hydrogens attached to carbon were placed at calculated positions and included in the refinement in the riding model approximation with $U_{iso}(H) = 1.2U_{eq}(C)$. Water and hydroxyl hydrogens were found in the difference-Fourier maps and refined with isotropic displacement parameters. One hydrogen attached to lattice water, O4w, is disordered over two positions with equal occupancy factors. The positions of O4w hydrogens were refined with the O–H and H···H distances constrained to 0.82 and 1.34 Å, respectively. Hydrogens attached to all remaining waters were freely refined. The summary of crystal data, experimental details, and refinement results are listed in table 1. Selected bond distances and angles are presented in table 2. The molecular plots were drawn with Mercury [29].

2.3. *Spectroscopy*

FT-IR spectra were recorded with an Equinox 55 spectrometer and analyzed from 400–4000 cm^{-1}. Samples in the solid state were measured in KBr pellets which were obtained with hydraulic press under 739 MPa pressure. Raman spectra of solid samples in capillary

Table 1. Crystal data and structure refinement details for $[Zn_4(C_9H_7O_3)_8(H_2O)_6]\cdot 4H_2O$.

Formula weight ($g\,M^{-1}$)	1746.81
T (K)	100(2)
Crystal system, space group	Triclinic, P-1
a (Å)	9.6667(4)
b (Å)	13.2050(7)
c (Å)	15.7465(7)
α (°)	108.638(4)
β (°)	100.742(3)
γ (°)	103.715(4)
V (Å^3)	1773.7(2)
Z	1
Calculated density ($g\,cm^{-3}$)	1.635
θ Range (°)	3.25–27.48
Absorption coefficient (mm^{-1})	1.433
Crystal size (mm)	$0.34 \times 0.22 \times 0.12$
Crystal color and form	Colorless block
Reflections collected/unique	8034/6678 [$R_{int} = 0.042$]
Final R indices ($I > 2\sigma(I)$)	$R_1 = 0.0453$; $wR_2 = 0.1125$
R indices (all data)	$R_1 = 0.0564$; $wR_2 = 0.1228$
Goodness-of-fit on F^2	1.044
Largest diff. peak and hole (e Å^{-3})	1.55/–0.81

Table 2. Selected bond lengths (Å) and angles (°) for $[Zn_4(C_9H_7O_3)_8(H_2O)_6]\cdot 4H_2O$.

Zn1–O1	2.109(2)	Zn1–O1w	2.081(2)
Zn1–O4	2.098(2)	Zn1–O2w	2.151(2)
Zn1–O7	2.072(2)	Zn1–O3w	2.124(2)
Zn2–O2$^{(i)}$	1.958(2)	Zn2–O8	1.947(2)
Zn2–O4	1.982(2)	Zn2–O10	2.002(2)
Zn1···Zn2	3.235(2)	Zn1···Zn2$^{(i)}$	5.301(2)
O7–Zn1–O4	92.20(8)	O1 W–Zn1–O4	173.49(8)
O1–Zn1–O4	89.19(7)	O3 W–Zn1–O2 W	168.70(8)
O7–Zn1–O1 W	92.83(8)	O8–Zn2–O4	110.24(8)
O1 W–Zn1–O1	86.29(8)	O8–Zn2–O10	101.58(8)
O7–Zn1–O3 W	84.48(8)	O4–Zn2–O10	103.82(8)
O1–Zn1–O3 W	89.11(8)	O8–Zn2–O2$^{(i)}$	117.83(8)
O4–Zn1–O3 W	86.22(8)	O2–Zn2–O4$^{(i)}$	117.07(8)
O1 W–Zn1–O3 W	98.38(8)	O2–Zn2–O10$^{(i)}$	103.67(8)
O7–Zn1–O2 W	86.43(8)		
O1–Zn1–O2 W	100.15(8)	O1–C1–O2	122.5(2)
O4–Zn1–O2 W	87.45(8)	O4–C10–O5	121.9(3)
O1 W–Zn1–O2 W	88.73(8)	O7–C19–O8	125.2(3)
O7–Zn1–O1	173.33(7)	O10–C28–O11	121.4(3)

Symmetry code: (i) $1 - x$, $1 - y$, $-z$.

tubes were recorded from 4000–100 cm^{-1} with a FT-Raman accessory of the Perkin-Elmer system 2000. The ^1H and ^{13}C NMR spectra of DMSO-saturated solutions were recorded with a Bruker Avance unit II 400 MHz at room temperature. Tetramethylsilane was used as an internal reference.

2.4. *Microbiological tests*

The solution of Zn(II) coumarate was prepared by dissolving 0.10 g of compound in 10% ethanol; the final mass of solution was 10.00 g. Micro-organisms *P. aeruginosa* (PCM

2270), *P. vulgaris* (PCM 2269), *S. aureus* (PCM 2267), *C. albicans* (PCM 2566), and *B. subtilis* (PCM 2021) were used for antimicrobial tests. The studied micro-organisms were inoculated on broth medium and stored at 37 °C (bacteria) or 25 °C (fungus) for 24 h. Then, 10.00 µl of prepared bacterial culture was added to 500.00 ml of sterile broth. 4.75 µl of broth inoculated with various strains of micro-organisms and 0.25 ml of Zn(II) *p*-coumarate solution were mixed in sterile test tubes. The concentration of tested compound in the test tube was 0.10%. Samples were incubated at 35 °C (bacteria) or 25 °C (fungus). The increase in the number of colonies was estimated similarly after 24 and 48 h of incubation for at least four samples. The growth of tested cells was standardized using turbidimetry method by measuring optical density at 600 nm with a UV-vis JASCO spectrophotometer. Statistical calculations were performed using Microsoft Office Excel 2010 [30].

3. Results and discussion

3.1. *Description of the crystal structure*

The chemical formula of the zinc complex (figure 1), as obtained from the single-crystal X-ray analysis, is $[Zn_4(C_9H_7O_3)_8(H_2O)_6]\cdot 4(H_2O)$. The compound is a centrosymmetric aggregate constructed from four Zn(II) cations, eight *p*-coumarate anions, and six waters. Additionally, two lattice waters are present in the asymmetric part of the crystal. Two crystallographically unique Zn(II) ions are connected by two carboxylates, bridging in the *syn*,*syn*-$\eta^1{:}\eta^1{:}\mu_2$ or $\eta^2{-}\mu_2$ fashion. The inversion-related Zn1/Zn2 subunits are further connected by adjacent *p*-coumarate which acts in the *syn*,*anti*-$\eta^1{:}\eta^1{:}\mu_2$ fashion. The coordination sphere of Zn1 is completed by three waters, resulting in a slightly distorted octahedral geometry. The Zn2 cation consists of four carboxylic oxygens from four

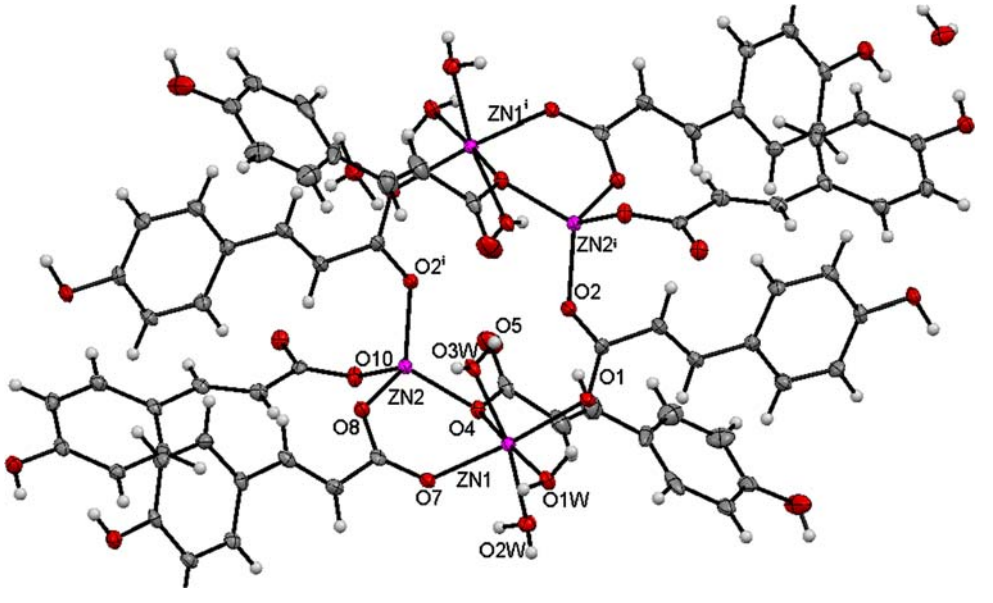

Figure 1. Perspective view of $[Zn_4(C_9H_7O_3)_8(H_2O)_6]\cdot 4(H_2O)$ with atom-numbering scheme. Thermal ellipsoids are drawn at the 50% probability level. Symmetry code: (i) 1–*x*, 1–*y*, –*z*.

different ligands and can be described as tetrahedral. The Zn–$O_{carboxyl}$ and Zn–O_{aqua} bond lengths are 1.947(2)–2.109(2) Å and 2.081(2)–2.151(2) Å, respectively (table 2), within the range of those observed for other four- or six-coordinate Zn(II) complexes with oxygen donors [31,32]. The distance of uncoordinated O5 from Zn2 is too long for effective interaction (Zn2···O5 = 2.866(2) Å). Adjacent Zn1···Zn2 ions are separated by 3.235(3) Å. Although the distance is indicative of some metal–metal interaction, it is too long to be considered as a bond [33,34]. All remaining Zn···Zn distances are much longer. Significant differences in the geometric parameters of four independent *p*-coumarates are observed. The most visible dissimilarity is in relative orientation of carboxylate with respect to the phenyl ring plane. As in the parent *p*-coumaric acid [35], in two molecules of the ligand carboxylates (O1−C1−O2 and O4−C10−O5) lie almost in planes of the benzene rings (the angles between appropriate best-planes are 8.3° and 8.5°, respectively). In two remaining ions, they are more twisted and form dihedral angles of 33.8° (O7−C19−O8) and 16.8° (O10−C28−O11) with appriopriate phenyl ring planes. The other difference is in the geometry of COO^- groups. Widening of the O−C−O angles in the bidentate-bridging carboxylates compared to values for monodentate is observed (table 2). Hydroxyl oxygens do not participate in coordination to zinc; however, they are involved in an extended net of strong intermolecular hydrogen bonds (figure 2, table 3) which link the tetranuclear $[Zn_4(C_9H_7O_3)_8(H_2O)_6]$ units into a complex 3D supramolecular network. Small channels are observable in the structure of the complex along the crystallographic [1 1 1] direction, filled with coordinated and lattice waters. The waters are hydrogen bonded to hydroxyl and carboxylate of the ligand.

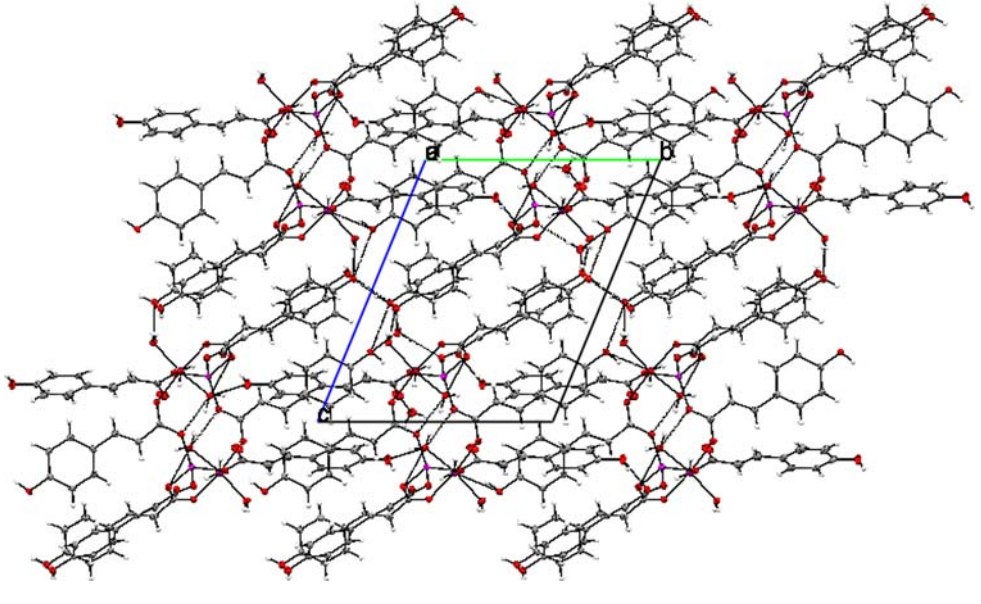

Figure 2. Part of the crystal structure of **1** along the *a* axis. Dashed lines indicate hydrogen bonds.

Table 3. Hydrogen-bonding geometry.

	D–H (Å)	H···A (Å)	D···A (Å)	<D–H···A (°)
O1w–H2w···O4w	0.82(2)	1.84(3)	2.648(3)	170(3)
O3w–H5w···O2	0.82(5)	1.86(2)	2.618(3)	154(2)
O12–H13o···O5w	0.84(3)	1.76(3)	2.591(2)	175(3)
O3–H3o···O1w$^{(ii)}$	0.89(4)	1.95	2.800(3)	160
O6–H6o···O11$^{(iii)}$	0.72(4)	1.92	2.635(3)	171
O9–H9o···O12$^{(iv)}$	0.83(4)	2.02	2.831(3)	167
O1w–H1w···O11$^{(v)}$	0.80(4)	1.89	2.688(3)	176
O2w–H3w···O12$^{(i)}$	0.78(4)	2.26	3.035(3)	174
O2w–H4w···O9$^{(vi)}$	0.80(4)	2.19	2.963(3)	165
O3w–H6w···O6$^{(vii)}$	0.83(4)	2.02	2.813(3)	160
O4w–H7w···O5$^{(v)}$	0.82(2)	1.95	2.750(3)	164
O4w–H8wa···O4w$^{(viii)}$	0.82(2)	2.02	2.824(3)	167
O4w–H8wb···O6$^{(ii)}$	0.82(2)	2.40	3.106(3)	145
O5w–H9w···O10$^{(i)}$	0.79(4)	2.03	2.792(3)	162
O5w–H10w···O3$^{(viii)}$	0.77(4)	2.12	2.861(3)	164

Symmetry codes: (ii) $2-x, 2-y, -z$; (iii) $1+x, 1+y, z$; (iv) $1-x, -y, 1-z$; (v) $1+x, y, z$; (i) $1-x, 1-y, 1-z$; (vi) $2-x, 1-y, 1-z$; (vii) $x, y-1, z$; (viii) $x, y-1, z+1$.

3.2. *FT-IR and FT-Raman*

The spectral assignments were done on the basis of literature data [36] and calculations executed for *p*-coumaric acid and sodium *p*-coumarate presented [37]. The numeration of the normal vibrations of benzene was done according to the notation used by Varsányi [38], ν stands for stretching vibrations, β for in-plane bending modes, γ for out-of-plane bending modes, φ(CC) for aromatic ring out-of-plane bending modes, α(CCC) for aromatic ring in-plane bending modes, ν_{as} means asymmetric, ν_s means symmetric, ν_{ar} stands for aromatic. The spectral assignment is presented in table 4; the FT-IR spectra of *p*-coumaric acid and Zn(II) *p*-coumarate, and the FT-Raman spectrum of zinc(II) complex are provided in Supplementary material.

Table 4. Selected wavenumbers from FT-IR and FT-Raman spectra of zinc(II) *p*-coumarate.

Wavenumbers [cm^{-1}]			Varsányi [38]	Wavenumbers [cm^{-1}]			Varsányi [38]
FT-IR	FT-Raman	Assignment		FT-IR	FT-Raman	Assignment	
3514 m		ν(OH)ar		1292 m	1303 vw	β(CH)c=c	
				1246 s	1249 m	νC-(OH)ar	
3350 m		ν(CH)ar		1223 s	1221 m	β(OH)ar	
3057 m	3064 vw	ν(CH)ar + ν(CH)c=c	20a	1173 s	1173 s	β(CH)ar	9a
3011 m	3026 vw	ν(CH)ar + ν(CH)c=c	20b	1107 m		β(CH)ar	18b
1640 s	1638 vs	ν(CC)c=c		1013 w	1015 vw	β(CH)ar	18a
1605 s	1607 vs	ν(CC)ar	8a	989 m-978 m	978 w	ν(CCO)	
1589 s		ν(CC)ar	8b	941 w		γ(CH)ar	17a
1545 s	1534 m	ν_{as}(COO$^-$)		866 m	866 m	γ(CH)	10a
1510 vs	1519 vw	ν(CC)ar	19a	835 s	838 vw	γ(CH)ar	17b
1458 m	1457 vw	ν(CC)ar	19b	802 m	806 m	α(CCC)	1
1408 s	1415 m	ν_s(COO$^-$)		718 w	721 vw	γ_s(COO$^-$)	
1389 s		β(CH)ar + β(OH)ar	14		645 w	φ(CC)	4
1348 s		β(CH)c=c		534 m		β_{as}(COO$^-$)	
1319 m	1321 wv	β(CH)c=c + β(OH)ar	3	517 m		φ(CC)	16b

The band derived from stretching hydroxyl group vibrations ν(OH) is located at 3514 cm^{-1}. At 3350–3011 cm^{-1} (IR) and 3064–3026 cm^{-1} (Raman) peaks assigned to stretching vibrations of CH from the aromatic ring and double bond between the ring and carboxylate ν(CH) are present. Bands assigned to C=C stretches of the double bond are at 1640 cm^{-1} (IR) and 1638 cm^{-1} (Raman). Four peaks characteristic for the aromatic system are 1605–1458 cm^{-1} (IR) and 1607–1457 cm^{-1} (Raman). Between 1389–1013 cm^{-1} (IR) and 1321–1015 cm^{-1} (Raman) bands assigned to in-plane deformations of CH β(CH) are present. At lower wavenumbers, peaks derived from out-of-plane deformations of CH γ(CH) are situated, i.e. 941–835 cm^{-1} (IR) and 866–838 cm^{-1} (Raman). Bands of in-plane and out-of-plane vibrations of the aromatic ring α(CCC) and ϕ(CC) are present at 802–517 cm^{-1} (IR) and 806–645 cm^{-1} (Raman). Peaks assigned to vibrations of carboxylate are $\nu_{as}(COO^-)$ 1545 cm^{-1} (IR) and 1534 cm^{-1} (Raman), $\nu_s(COO^-)$ 1408 cm^{-1} (IR) and 1415 cm^{-1} (Raman), $\gamma_s(COO^-)$ 718 cm^{-1} (IR) and 721 cm^{-1} (Raman), and $\beta_{as}(COO^-)$ 534 cm^{-1} (IR).

3.3. *^{1}H and ^{13}C NMR*

The chemical shifts from ^{1}H and ^{13}C NMR spectra of zinc *p*-coumarate as well as *p*-coumaric acid [28] are gathered in table 5. A comparison of the ^{1}H and ^{13}C NMR spectra of the *p*-coumaric acid with those of zinc *p*-coumarate points at the absence of the carboxylic -OH signal (12.13 ppm in ligand) and a shift in the peak position derived from H2, H6 ($7.33_{complex}$; 7.49_{acid} ppm), and H8 ($7.38_{complex}$; 7.52_{acid} ppm) indicates bonding between

Table 5. Chemical shifts from of ^{1}H and ^{13}C NMR spectra of zinc *p*-coumarate and *p*-coumaric acid, δ [ppm].

Atom numbering	Zn(II) *p*-coumarate 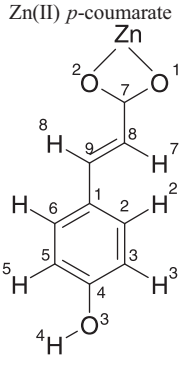	*p*-Coumaric acid [37] 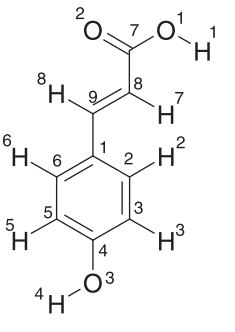
H1	–	12.13
H2 and H6	7.33	7.49
H3 and H5	6.75	6.79
H4	9.93	9.96
H7	6.30	6.29
H8	7.38	7.52
C1	126.11	125.36
C2 and C6	129.24	130.17
C3 and C5	120.65	115.83
C4	158.85	159.67
C7	172.12	168.05
C8	115.71	115.41
C9	140.96	144.27

Table 6. The degree of growth inhibition of *B. subtilis*, *C. albicans*, *P. aeruginosa*, *P. vulgaris,* and *S. aureus* caused by zinc(II) *p*-coumarate after 24 and 48 h of incubation [13].

Micro-organism	Incubation [h]	Zinc *p*-coumarate
S. aureus	24	77 ± 3
	48	75 ± 2
P. vulgaris	24	68 ± 3
	48	4 ± 10
C. albicans	24	63 ± 4
	48	65 ± 7
B. subtilis	24	34 ± 12
	48	52 ± 5
P. aeruginosao	24	7 ± 17
	48	6 ± 7

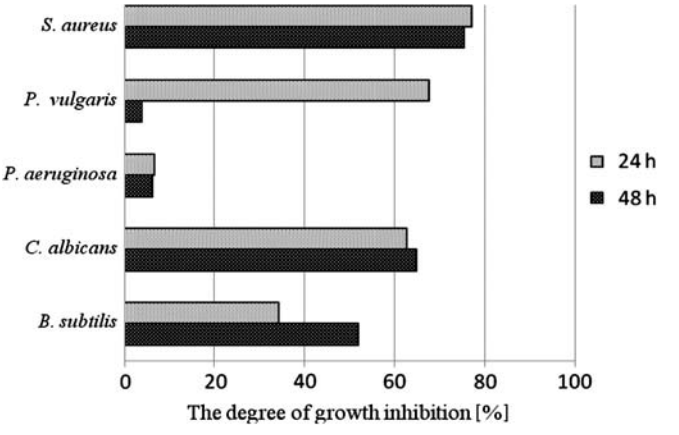

Figure 3. The degree of growth inhibition of *B. subtilis*, *C. albicans*, *P. aeruginosa*, *P. vulgaris,* and *S. aureus* by zinc *p*-coumarate.

carboxylate of *p*-coumaric acid and zinc, and changes in the electronic charge distribution of molecule caused by complex formation. Significant changes in appropriate peak position are observed in the ^{13}C NMR spectra of Zn complex and ligand for signals assigned to C3, C5 ($120.65_{complex}$; 115.83_{acid} ppm), C7 ($172.12_{complex}$; 168.05_{acid} ppm), and C9 ($140.96_{complex}$; 144.27_{acid} ppm) atoms.

3.4. *Microbiology*

Zinc(II) p-coumarate with 0.1% concentration (in broth culture) shows different effects on the growth of selected strains of *E. coli*, *P. aeruginosa*, *B. subtilis*, *S. aureus* and *P. vulgari* and fungus *C. albicans* after 24 and 48 h of incubation (table 6, figure 3). Zn *p*-coumarate possesses the strongest antimicrobial properties toward *S. aureus*, *P. vulgaris,* and *C. albicans,* although, for *P. vulgaris,* the antibacterial activity of Zn *p*-coumarate decreases after 48 h of incubation. The reverse situation for *B. subtilis* was shown, i.e. Zn *p*-coumarate causes higher inhibition of bacteria growth after 48 h than after 24 h of incubation. Tested compound possesses weak antibacterial activity toward *P. aeruginosa*.

4. Conclusions

The synthesis of single crystals of a zinc(II) complex of *p*-coumaric acid was described. The single-crystal X-ray analysis shows that in contrast to zinc(II) *trans*-cinnamate dihydrate [39], which exists in the form of simple monomers with six-coordinate metal, the studied complex is a tetranuclear aggregate with two different metal centers. Significant differences in the geometric parameters of four independent *p*-coumarates were observed. The FT-IR, FT-Raman, ^{1}H and ^{13}C NMR spectra for Zn(II) *p*-coumarate were analyzed. A decrease in the chemical shifts of all protons in ^{1}H NMR spectrum of complex in comparison to appropriate chemical shifts in the spectrum of ligand points at an increase in screening of aromatic protons in zinc *p*-coumarate molecule as a consequence of the circular current weakening. The substitution of zinc in the carboxylate of *p*-coumaric acid causes the most significant changes in the electronic charge distribution around C7, C9, C5, and C3. The obtained spectral characteristics are good parameters for statistical correlation between molecular structures of studied compounds and their biological activity. Tested compound has potential application as an antimicrobial agent with biological activity toward selected micro-organisms. Zn *p*-coumarate possesses high antimicrobial activity against *S. aureus*, *P. vulgaris,* and *C. albicans,* and weak antibacterial properties toward *P. aeruginosa*.

Supplementary data

CCDC 885438 contains the supplementary crystallographic data for the structure reported in this article. Copies of available materials can be obtained free of charge on application to CCDC, 12 Union Road, Cambridge CB2 1EZ, UK (Fax: +44 1223 336 033; E-mail: data_request@ccdc.cam.ac.uk or www: http//www.ccdc.cam.ac.uk/data_request/cif).

Acknowledgment

Scientific work was financed from the budget for science in 2010–2013 as a research project of Ministry of Science and Higher Education, Poland, no. N N305 384538. The authors would like to thank prof. Izabela Święcicka for the opportunity of microbiological measurements that were carried out in the Department of Microbiology, Institute of Biology, University of Bialystok, Poland.

References

[1] N. Balasundram, K. Sundram, S. Samman. *Food Chem.*, **99**, 191 (2006).
[2] U.Y. Shaheen. *Free Rad. Antiox.*, **1**, 23 (2011).
[3] P. De, M. Baltas, F. Bedos-Belval. *Curr. Med. Chem.*, **18**, 1672 (2011).
[4] A. Wen, P. Delaquis, K. Stanich, P. Toivonen. *Food Microbiol.*, **20**, 305 (2003).
[5] B.N. Lenta, B. Weniger, C. Antheaume, D.T. Noungoue, S. Ngouela, J.C.N. Assob, C. Vonthron-Sénécheau, P.A. Fokou, K.P. Devkota, E. Tsamo, N. Sewald. *Phytochemistry*, **68**, 1595 (2007).
[6] A. Garcia-Ruiz, B. Bartolomé, A.J. Martinez-Rodriguez, E. Pueyo, P.J. Martin-Álvarez, M.V. Moreno-Arribas. *Food Control*, **19**, 835 (2008).
[7] O. Escuredo, L.R. Silva, P. Valentão, M.C. Seijo, P.B. Andrade. *Food Chem.*, **130**, 671 (2012).
[8] S.F. Bodini, S. Manfredini, M. Epp, S. Valentini, F. Santori. *Lett. Appl. Microbiol.*, **49**, 551 (2009).
[9] S. Smolarek, A. Vdovin, D.L. Perrier, J.P. Smit, M. Drabbels, W.J. Buma. *J. Am. Chem. Soc.*, **132**, 6315 (2010).

[10] S.M. An, J.S. Koh, Y.C. Boo. *Phytother. Res.*, **24**, 1175 (2010).
[11] D. Vauzour, G. Corona, J.P.E. Spencer. *Arch. Biochem. Biophys.*, **501**, 106 (2010).
[12] S.I. Lee, S.M. An, G.I. Mun, S.J. Lee, K.M. Park, S.H. Park, Y.Ch. Boo. *J. Appl. Biol. Chem.*, **51**, 148 (2008).
[13] M. Kalinowska, J. Piekut, W. Lewandowski. *Corrosion Protection*, 9s/A, 309 (2012).
[14] W.N. Setzer, M.C. Setzer, R.B. Bates, P. Nakkiew, B.R. Jackes, L. Chen, M.B. McFerrin, E.J. Meehan. *Planta Med.*, **65**, 747 (1999).
[15] J. Hoffmanova, A. Kozubik, L. Dusek, J. Pachernik. *Eur. J. Pharmacol.*, **350**, 273 (1998).
[16] M. Manjunathay, V.H. Naikz, A.D. Kulkarniz, S.A. Patil. *J. Coord. Chem.*, **64**, 4264 (2011).
[17] S. Budagumpi, U.N. Shetti, N.V. Kulkarni, V.K. Revankar. *J. Coord. Chem.*, **62**, 3961 (2009).
[18] S.A. Patil, S.N. Unki, A.D. Kulkarni, V.H. Naik, U. Kamble, P.S. Badami. *J. Coord. Chem.*, **64**, 323 (2011).
[19] L. Dawara, R.V. Singh. *J. Coord. Chem.*, **64**, 931 (2011).
[20] H. Li, C.W. Hu. *J. Solid State Chem.*, **177**, 4501 (2004).
[21] J. Yan, Y. Guo, H. Li, X. Sun, Z. Wang. *J. Mol. Struct.*, **891**, 298 (2008).
[22] G.B. Deacon, M. Forsyth, P.C. Junk, S.G. Leary, W.W. Lee. *Z. Anorg. Allg. Chem. (J. Inorg. Gen. Chem.)*, **635**, 833 (2009).
[23] J.-Y. Mao, H.-X. Fang, Q-F. Xu, Q.-X. Zhou, J.-M. Lu, Y. Zhang. *Wuji Huaxue Xuebao (Chin.) (Chin. J. Inorg. Chem.)*, **24**, 1046 (2008).
[24] Q.-F. Xu, Q.-X. Zhou, J.-M. Lu, X.-W. Xia, Y. Zhang. *J. Solid State Chem.*, **180**, 207 (2007).
[25] V. Zelenak, I. Cisarova, P. Llewellyn. *Inorg. Chem. Commun.*, **10**, 27 (2007).
[26] CrysAlis CCD and CrysAlis RED, Oxford Diffraction Ltd., Abingdon, UK (2006).
[27] G.M. Sheldrick. *Acta Cryst. A*, **64**, 112 (2008).
[28] L.J. Faruggia. *J. Appl. Crystallogr.*, **32**, 837 (1999).
[29] C.F. Macrae, P.R. Edgington, P. McCabe, E. Pidcock, G.P. Shields, R. Taylor, M. Towler, J. van de Streek. *J. Appl. Cryst.*, **39**, 453 (2006).
[30] Microsoft Office Excel, Microsoft (2010).
[31] R.P. Davies, R.J. Less, P.D. Lickiss, K. Robertson, A.J.P. White. *Inorg. Chem.*, **47**, 9958 (2008).
[32] A. Waheed, R.A. Jones, J. McCarty, X. Yang. *Dalton Trans.*, 3840 (2004).
[33] G. Parkin. *Science*, **305**, 1117 (2004).
[34] I. Resa, E. Carmona, E. Gutierrez-Puebla. *Science*, **305**, 1136 (2004).
[35] R.F. Bryan, P.G. Forcier. *Mol. Cryst. Liq. Cryst.*, **60**, 157 (1980).
[36] M. Kalinowska, R. Świsłocka, W. Lewandowski. *J. Mol. Struct.*, **834–836**, 572 (2007).
[37] R. Świsłocka, M. Kowczyk-Sadowy, M. Kalinowska, W. Lewandowski. *Spectrosc.*, **27**, 35 (2012).
[38] G. Varsányi. *Assignments for Vibrational Spectra of 700 Benzene Derivatives*, Akademia Kiado, Budapest (1973).
[39] H. Hosomi, S. Ohba, Y. Ito. *Acta Cryst.*, **C56**, e123 (2000).